Title
A STEM X-RAY MICROANALYTICAL STUDY OF PHOSPHORUS SEGREGATION TO GRAIN BOUNDARIES IN THIN-FILM SILICON

Author
Rose, J.H.

Publication Date
1982-06-01

Lawrence Berkeley Laboratory
UNIVERSITY OF CALIFORNIA

Materials & Molecular Research Division

A STEM X-RAY MICROANALYTICAL STUDY OF PHOSPHORUS SEGREGATION TO GRAIN BOUNDARIES IN THIN-FILM SILICON

Jamie H. Rose
(M.S. thesis)

June 1982

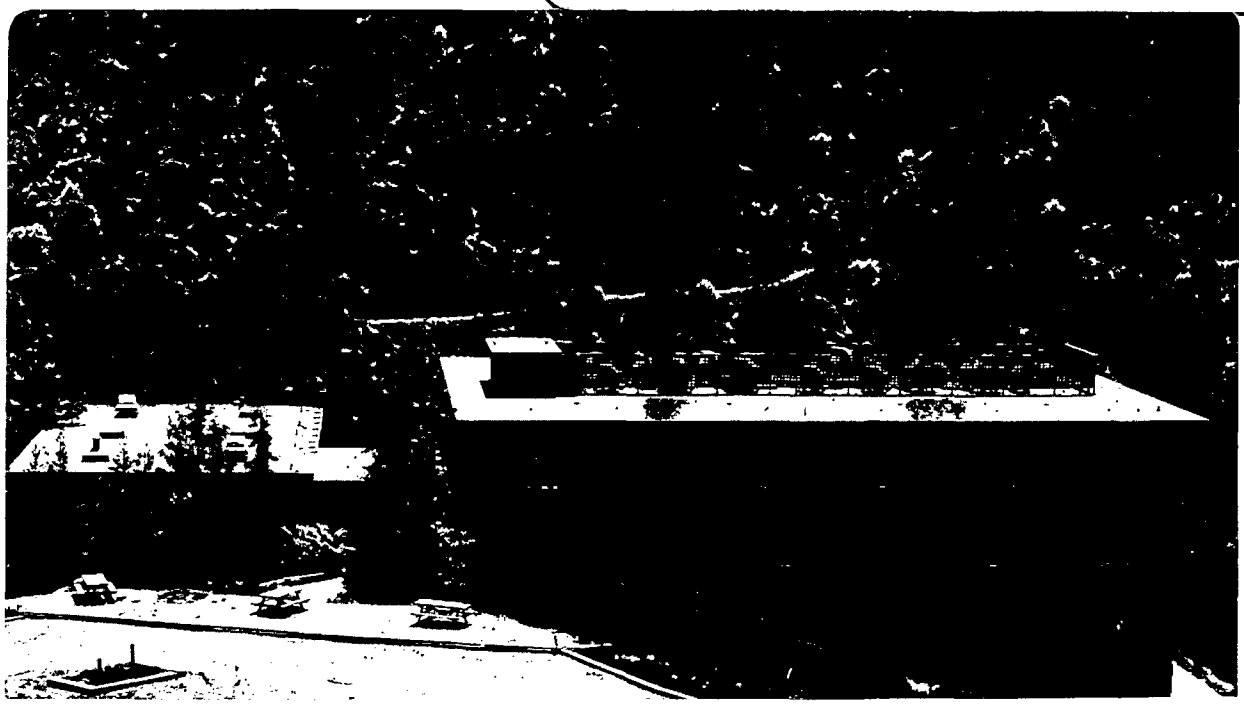

Prepared for the U.S. Department of Energy under Contract DE-AC03-76SF00098

DISCLAIMER

A STEM X-RAY MICROANALYTICAL STUDY OF PHOSPHORUS SEGREGATION TO GRAIN BOUNDARIES IN THIN-FILM SILICON

Jamie H. Rose

Department of Materials Science and Mineral Engineering

University of California

and

Materials and Molecular Research Division

Lawrence Berkeley Laboratory

Berkeley, California 94720

Master of Science Thesis

June 1982

This work was supported by the Director, Office of Energy Research, Office of Basic Energy Sciences, Materials Science Division of the U. S. Department of Energy under Contract No. DE-AC03-76SF00098.

Abstract

STEM X-ray microanalysis has been applied in the characterization of phosphorus segregation to individual grain boundaries in thin-film silicon. Heavily doped material annealed between 650°C and 800°C was examined. The extent of segregation varied from boundary to boundary in a given sample. This lead to an average segregation energy of 7.5 Kcal/mole. Using the coincident site lattice model of grain boundary structure, the amount of segregation for a few boundaries was correlated with boundary type. It appears that geometrical models may have some basis for predicting structural and energetic features of diamond structure materials.

Table of Contents

I. Introduction	1
II. Experimental Considerations	2
A. Material Studied	2
B. TEM	3
C. STEM Microanalysis of Grain Boundaries	3
D. Axis-Angle Pair Determination	6
III. Results	7
A. Auger Analysis	7
B. TEM	7
C. STEM Microanalysis	8
D. Axis-Angle Pairs	9
IV. Discussion	9
A. Correlation of Segregation with GB Structure	9
B. Thermodynamic Considerations	11
V. Conclusions	13
Appendices	14
Acknowledgements	18
References	19
Tables	22
Figure Captions	25
Figures	26

I. Introduction

Due to the many applications of chemically vapor-deposited polycrystalline silicon in integrated circuit technology and inexpensive solar cells, its properties have been studied extensively during the past ten years. The grain boundaries (GB) in this material distinguish it from single-crystal silicon (aside from the relative crystal misorientation from grain to grain). Thus, all this research aims at elucidating the electronic properties of the GB's. It is important to appreciate how difficult a problem this is in solid state physics: truly fundamental understanding of the problem cannot be expected until the subject of defects in crystals has progressed beyond its infancy. Nonetheless, the basic properties of thin-film polycrystalline silicon (referred to as polysilicon by industry) are well-documented and may be explained by simple, approximate models.

Workers in this field generally fail to acknowledge the foundations for their research. It has long been recognized that lattice defects in a semiconductor, in addition to dopants, introduce states in the band gap. In particular, the basic features of GB's were elucidated approximately thirty years ago.[1-3] Current models of polysilicon essentially extend these notions about individual GB's to geometrically idealized models of polysilicon.

These models should consider two salient features of semiconductor GB's: they induce defect states in the band gap which may serve to capture majority carriers and they may exhibit segregation of the dopant species, possibly electrically neutralizing these atoms. Until recently, only the former effect had been considered in any detail.[4-6] This is not surprising since the subject of grain boundary segregation is more familiar to metallurgists than to electrical engineers.

This thesis describes an investigation of dopant segregation to silicon GB's, a field in which but a few papers have appeared.[7-11] Some of this work infers segregation by examining properties which it affects (e.g. resistivity) while all utilize techniques which average over the effect of many GB's (and possibly other defects in the material). The present study aims to obtain direct information from individual GB's by use of fine probe STEM/X-ray microanalysis. The intent is to present direct proof of phosphorus segregation to silicon GB's and correlate segregation properties with the structure of individual GB's.

Note that our attention is limited to equilibrium as opposed to non-equilibrium segregation. The former occurs within a few atomic layers of the interface, serving to reduce GB energy. The latter is associated with phenomena such as interfacial movement and forced diffusion and may extend for several hundred angstroms beyond the GB.

II. Experimental

A. Material Studied

CVD silicon was selected for this study due to its wide technological applications. Due to the solute concentration detection limits of X-ray microanalysis, it was additionally decided to examine heavily doped material. Specifically, the original material consisted of wafers coated with 2750Å of silicon by the LPCVD (low-pressure, chemically vapor-deposited) process and heavily phosphorus doped via a cycle of 40 minutes at 950°C in PH_3.

This material was sputter-coated with 1500Å of SiO_2 (to prevent out-diffusion) and divided into several pieces for various annealing treatments given

in Table 1. For the heat treatments, the samples were sealed in quartz ampules in an argon atmosphere. This allowed use of the available metallurgical furnaces.

TEM specimens were prepared from each sample. 3mm discs were cut with an impact drill, mechanically thinned to about 5 mils, chemically thinned from the back side to a point near perforation (with a solution of 1 HF: $2CH_3$: $3HNO_3$), and finally ion-milled. This minimized preferential etching at the GB's.

B. Transmission Electron Microscopy

TEM provided a survey of defects in the polysilicon. It was particularly used to search for precipitates which potentially could nucleate at GB's and/or remove phosphorus from substitutional lattice sites reducing the effective concentration of phosphorus in the matrix.

C. STEM Microanalysis of Grain Boundaries

A Philips EM400 (LaB_6 filament) equipped with a Kevex energy dispersive spectrometer was operated in STEM mode. This instrument has a 40Å minimum probe diameter.

The STEM work in this study is in part an exercise in pushing the technique to the limits of its usefulness. Getting the most from this method is first a geometrical problem. As depicted in Fig. 1, the STEM probe is sampling the portion of a GB which intersects the probe. To simplify, we may consider the GB to be a nearly two-dimensional defect (GB thickness is on the order of 10Å).[12,13] The probe thus samples GB material and adjacent grain material which dilutes the signal due to any segregation at the GB. The optimum case has the GB plane perfectly parallel to the probe and the probe exactly centered on the GB. For a 40Å diameter probe, assuming no beam spreading, and a GB thickness of 10Å , the ratio of grain to GB in the probe is 2.14. Any

experimental situation will easily be much worse than this. Salient factors are: ANGULAR DISPLACEMENT OF BEAM AND GB--a beam misalignment of 2.3° in the above case will just allow the "top" and "bottom" of the GB to lie in the probe. In other words, as the GB plane tilts from the probe its "signal" decreases; TRANSLATIONAL DISPLACEMENT OF PROBE AND GB--for a GB projected width of 40Å and a probe diameter of 40Å, perfect alignment is clearly impossible. Specimen drift is an important factor here (probe placement must be checked every 10-20 seconds while acquiring a spectrum). In addition, there is a small displacement between the probe on the STEM CRT and the actual probe position on the foil, leading to another source of inaccuracy; and BEAM SPREADING--Monte Carlo calculations and experimental estimations indicate significant beam spreading,[14] but there is reason to doubt these findings. The former employ scattering models which may not accurately depict the physical situation, while the latter are subject to the errors introduced by the factors discussed above. Recent experimental observations suggest beam spreading due to inelastic scattering is negligible in reasonably thin foils[15] (about 1500Å thick). It is possible, however, to quantify beam spreading due to the angular convergence of the probe by a simple geometrical analysis. In the EM400, utilizing the second condenser aperture, this angle is experimentally found to be 3.6°. In a 1500Å thick foil, the effective beam broadening is 24Å, a relatively small correction to the 100Å probe used in the experimental work.

Practically, visual placement of a 40Å or 100Å probe on a GB is likely very inaccurate. The convergent beam diffraction pattern appearing in the microscope while in STEM mode allows much greater precision for positioning the probe. This method is not only recommended, but likely a necessity.

The second experimental feature important to this study is the small phosphorus concentration being examined. Phosphorus is detectable to approximately .2 at% (see Appendix A): with the dilution effect previously considered, the excess P concentration measured with the probe on a GB is on this order (and for heavily doped material only slightly above the background concentration). Thus, statistical considerations figure heavily into data analysis. Spectra here characteristically exhibit a strong Si peak with a slight P "peak" on its shoulder (Fig. 2). The concentration difference between GB and grain is generally not observable by eye.

The problem then is to extract the P peak counts. The approach employed is to acquire a GB spectrum over several minutes, moving the probe along the GB. A second spectrum is then acquired, scanning the probe over a small region surrounding the GB of interest. The number of counts in the second spectrum is increased over the first so that its counting error is small relative to the first spectrum. The second spectrum is then subtracted from the GB spectrum after normalizing. The number of counts in an appropriately selected window about the P peak are then due to P atoms segregated at the GB. This method of background subtraction is normally impossible, since the shape of the background varies and the relative peak heights change greatly with different concentrations. Here though, the slight P concentration variation will have negligible effect.

Finally, the random counting error in the P peak is proportional to the square root of the total counts in the P peak window (including background) in the original GB spectrum. This large source of error may only be minimized with long counting time and by maximizing beam current with the largest condenser aperture and/or increasing filament bias. Statistical considerations are given in Appendix B.

In practice, the specimen is loaded in a low-background holder which has a single tilt degree of freedom. This must be set approximately 30° toward the detector to maximize collected X-rays. This limitation combined with the very small grain size of the material ($\gtrsim$ 500Å diameter) complicates vertical alignment of a GB. One must examine a region of the foil until finding a suitable boundary, tilting somewhat to bring the grains into contrast. A projected GB width of 100Å is the best regularly obtainable, this being chosen as a standard.

D. Axis-Angle Pair Determination

As a test of the applicability of coincident site lattice (CSL) theory to silicon GB's (see IVA), microdiffraction was employed to evaluate the type of GB (i.e. near coincident versus general GB) in a few cases. This is done by first finding the axis-angle pair for the GB. The relative orientation of any two grains may be given in terms of a common crystallographic axis and a rotation about this axis. This axis-angle pair is evaluated from two pairs of diffraction patterns taken from the relevant grains, before and after tilting the specimen. Details may be found in Ref. 16. The CSL is then found by comparing with tables of CSL's and their associated axis-angle pairs.[17] How close an axis-angle pair must be to an exact coincident orientation to be considered a "special" or well-ordered GB is open to debate. We use the criterion that the boundary must be within ϕ degrees of an exact CSL orientation, where $\phi = 15° \Sigma^{-1}$ (Ref. 18). Σ^{-1} is the fraction of shared lattice sites for a given CSL.

III. Results

A. Auger Analysis

Since estimates of phosphorus diffusivity at the high concentrations and relatively low temperatures employed are speculative, Auger depth concentration profiles indicated the extent of diffusion in the annealed specimens (e.g. Fig. 3). These profiles exhibit a fairly uniform concentration, while showing that extensive diffusion has occurred. On this basis, an approximately equilibrium condition of the material for thermodynamic considerations is assumed. The phosphorus concentration in the thin film is .6% $\pm$ .2%. This variation is acceptable since the level of segregation is a weakly varying function of the matrix phosphorus concentration (Appendix C). Also note that for the 650°, 700°, and 750°C anneals, the polysilicon remains supersaturated. This complicates the thermodynamic analysis as discussed below.

B. TEM

Fig. 4 is a typical micrograph. Grain size is in the range ~ 500Å - 2000Å. Many stacking faults are present. No structure was visible in the GB's, with one exception: a single boundary exhibited a dislocation structure typical of a low angle boundary (Fig. 5).

Three distinct possible precipitates are observed. Some of the annealed and chemically thinned specimens exhibited round, precipitate-like objects approximately 200Å across (Fig. 6). These were removed by ion-milling and so are likely a surface effect due to the chemical etching of heavily doped and annealed silicon.

The material annealed at 650°C and 700°C also contained a few objects exhibiting dislocation loop type contrast (Fig. 7). These may originate from vacancy or interstitial condensation or may be phosphorus atom platelets.

Assuming the final possibility to be true, there are too few to significantly alter the concentration of phosphorus atoms in substitutional lattice positions.

The third feature appears as dark spots approximately 25Å across. These are present at all annealing temperatures and in the unannealed silicon (Fig. 8). Similar appearing defects have been observed in arsenic doped silicon where it is suggested that they are arsenic atom clusters.[36] Mandurah et al.[9], in an investigation of arsenic segregation in LPCVD silicon via resistivity measurements, addressed the question of arsenic atom clustering in their specimens. They examined material of three different average arsenic concentrations, .4%, .12%, and .04%, the first being about the same as the phosphorus concentration in this study. Though clustering would likely be significant at .4%, no anomalous behavior was observed. We thus assume for the present study that phosphorus clustering is not affecting the extent of GB segregation.

C. STEM/Microanalysis

Since observations were near or below the limits of detectability of phosphorus in a silicon matrix, it was very important to optimize all factors during data acquisition. In particular, probe current and acquire time were increased to their practical limit. Still, error was very large, limiting the quantitative potential of this work. In Table II, the raw data for GB's observed are given (i.e. listed by annealing temperature with silicon peak counts and GB phosphorus excess counts presented and standard deviation, σ, for the latter as discussed in IIC). The time of data collection for each observation varied with GB length, contamination rate, and operator experience. The surface excess concentration is also given, in units of a (100) monolayer [6.8×10^{14} cm^{-2}], by use of the Cliff-Lorimer method for quantification of the X-ray data[14] and a simple geometrical analysis, as described by Doig and Flewitt,[37] to convert excess

phosphorus observed by the probe to the excess phosphorus concentration at the GB. Note the error inherent in the measurements (σ versus PKα) and the variation in amount of segregation (last column).

D. Axis-Angle Pairs

Axis-angle pairs were determined for six GB's which exhibited varying levels of segregation. This small number is due to the difficulty and time consuming nature of the analysis on such fine-grained material: the STEM microdiffraction pattern has a small angular extent while it is generally impossible to tilt to an easily recognizable orientation. These GB's are listed in Table III where Σ and its associated axis-angle pair are given for the nearly coincident boundaries. Note that the nearly coincident boundaries exhibit lower levels of phosphorus than do the random GB's.

IV. Discussion

A. Correlation of Segregation with GB Structure

The most obvious conclusion of this study is that phosphorus segregates to silicon GB's under appropriate conditions (this only being indirectly proven until now). More intriguing, though, is the observation that segregation varies from GB to GB. This clearly suggests a variation in GB structure, something completely ignored in previous studies which employed techniques averaging over the effect of many GB's (e.g. Hall effect or resistance measurements).[7-11]

A salient question then is what may reasonably be said about GB structure in silicon. Our sources are essentially based on studies of metals in which non-directional bonding and a single atom basis has provided a foundation for extensive work utilizing geometrical models. Notably, Bollmann's "O-lattice" theory provides a basis for predicting structural features of a given GB, based on a knowledge of the relative orientation of the two grains and the particular

GB plane.[19,20] The remarkable success of this theory is well documented in metals.[13,21] However, the situation in semiconductors is complicated by strong directional bonding and electronic effects which may be expected to obviate the use of a geometrical theory that only takes the lattice in question into account. Relatively little work has been done on the structure of semiconductor grain boundaries (low-angle, dislocation array boundaries are an exception).[21-25].

A general silicon GB could consist of a disordered layer independent of the relative orientation of the neighboring lattices. In the first systematic study of silicon GB structure, the predicted secondary dislocations of O-lattice theory were not observed in a $\Sigma = 5$ boundary.[25] However, since this work, theoretical and experimental studies have appeared confirming various aspects of this theory in semiconductors. Möller[26] has demonstrated (for <110> tilt boundaries) that several coincident orientations lead to lower energy configurations than that for a random GB. These reduced energy structures are possible since germanium and silicon bonds may bend ~ 25° before breaking (i.e. forming a dangling bond). This factor was long ago employed by Hornstra[27] to model diamond structure dislocations with a minimum of dangling bonds. Experimentally, secondary dislocations have been observed in several different boundaries in germanium.[28-30] It thus appears that geometrical models provide at least a partial basis for predicting semiconductor GB structure and energy and, consequently, susceptibility to segregation. The basic notion is that highly disordered GB's provide reduced energy sites for segregated atoms--and have more potential for energy reduction--than do GB's near coincident orientations which exhibit good matching. A limited amount of experimental work supporting this expected behavior exists, entirely for metals.[18,31,32] Though systematic and quantitative data are lacking, the evidence clearly indicates substantially reduced segregation at near coincident and low angle (i.e. near $\Sigma = 1$) GB's.

Relating this to the present study, we note in Table III that the low-angle and twin boundaries (known to be well-matched) exhibit low segregation, as expected. The two random boundaries have a relatively high degree of segregation. Most significant though are the two near coincident boundaries which evince minimal segregation. This supports the contention that CSL theory can predict well-ordered GB's in semiconductors, simultaneously indicating that this is a basis for predicting segregation behavior. No hard conclusions may be drawn, though, due to the error in the measurements and the limited data. Clearly, further research on a material more amenable than polysilicon is warranted.

B. Thermodynamic Considerations

A few caveats must first be mentioned concerning analysis of segregation in semiconductors. Though our heavily doped material is dilute by metallurgical standards (< 1%), silicon doping of .01% or more causes significant structural and electronic effects.[33] Aggregates of dopant atoms, dopant and silicon atoms, or dopant atoms and vacancies may form, while the large strain has long been known to produce dislocations.[34] The dopant may also interact with oxygen in the polysilicon. These possibilities were considered in IIIB.

Thermodynamic theories of segregation cannot take details of GB structure into account, but our lack of such information obviates this concern. It is clear, though, that the structural changes lead to a variation in the heat of adsorption among GB's, while also likely leading to a range of values for a given GB (depending on the specific environment of an adsorbed atom). Since we have no data concerning the latter, a GB is here assumed to have a single energy value which may be thought of as an average over its available sites.

A simple model appropriate to this study (as outlined in Appendix C) gives:

$$C_{GB} = \frac{C\, e^{Q/RT}}{1 + Ce^{Q/RT}}$$

where C_{GB} is the concentration of phosphorus at GB sites, C is the matrix concentration of phosphorus, and Q is the free energy of segregation. Experimentally, we have C and C_{GB} as a function of temperature (assuming a GB width of 10Å). Clearly, Q is a function of GB type as indicated in the previous section. The above equation then yields a family of curves with Q as a parameter.

The data may best be interpreted as exhibiting a maximum and a minimum Q. Several GB's exhibit no segregation above the detection limit at all temperatures studied, this providing an upper limit for Q_{min}. We may also use the GB's with maximum segregation to set an upper limit on Q. Choosing C_{GB} = 1 to correspond to 6.8×10^{14} cm^{-2} (the atomic density of a (100) plane)* we find that

$$Q_{max} = 10 \frac{Kcal}{mole}$$

$$Q_{min} \leq 5 \frac{Kcal}{mole} .$$

In Fig. 9 a curve is fitted to the average values for segregation at each temperature. This gives

$$\bar{Q} = 7.5 \frac{Kcal}{mole} .$$

---

*A saturated GB contains approximately one monolayer of solute.[13]

This compares reasonably well with the value of 10.2 $\frac{Kcal}{mole}$ found by Mandurah et al.[9] They examined phosphorus segregation via resistivity measurements in material doped by ion implantation and annealing to yield an average concentration of .04%, about one tenth the value in this study. The material was evaluated for annealing temperatures in the range 800°C to 1000°C, this contiguous to the range examined here. Further studies are required to specify the source of the discrepancy.

V. Conclusions

Phosphorus segregation to silicon GB's exhibits a large variation at a given annealing temperature from which is deduced a corollary variation in boundary structure. It appears that a basis exists for predicting some segregation properties--and hence structural features--utilizing geometrical GB models. Further systematic work is suggested on relatively large grained material (one micron to bicrystal).

When modeling the electronic properties of polycrystalline silicon, one must take account of the thermal history of the silicon, applying segregation theory to find the number of dopant atoms at GB's. The assumption of dopant neutralization at GB's may then be applied. For more detailed understanding, further studies on the electronic and physical structure of silicon GB's are required, including consideration of possible changes in the electronic defect states concomitant with the type and level of dopant at the GB.

The limited applicability of STEM microanalysis to semiconductor problems is evident. Clearly, work in this field must be carefully selected if fruitful results are to be expected.

Appendix A

Detection Limits

The detection limit of an element in a matrix is generally expressed as a minimum mass fraction (MMF).[14] Since theoretical estimates of MMF are somewhat questionable, it seems best to express MMF in terms of spectra obtained with the instrument employed in the data collection. We take as a minimally significant phosphorus peak $N = 3(2N_{BKG})^{1/2}$, where N is the minimum detectable number of phosphorus counts and N_{BKG} is the number of counts in the continuum under the phosphorus peak. For a spectrum with 2×10^5 silicon peak counts, this gives MMF = .17%. For 4×10^4 counts, it becomes .37%.

Our ability to measure variations in concentration is somewhat better than this. This is accomplished, as described in IIB, by reducing the error in the reference spectrum where a larger probe and hence much higher counting rate may be utilized.

Appendix B

Error Analysis

Absorption effects are assumed to be negligible. It is assumed that error is dominated by the random nature of the X-ray production process. The error in counts attributable to segregated atoms is taken to be:

$$\sigma^2 = N_{GB}^{P} + \left[\frac{N_{GB}^{Si}}{N^{Si}}\right]^2 N^{P}$$

where N_{GB}^{P} is the number of counts in the phosphorus peak (including background) for the GB spectrum, N^{P} is this value in the corresponding matrix spectrum, and N_{GB}^{Si} and N^{Si} are the related silicon peak counts.

Appendix C

Thermodynamic Model of GB Segregation

Due to the semi-quantitative nature of the data, a simple model as outlined by McLean[35] is applied. The free energy of solute atoms is

$$G = PE + pe - KT \ln \Omega$$

$$\Omega = \ln n!\, N!\, - \ln(n-p)!\, p!\, (N-P)!\, P!$$

where E is the energy of a solute atom at a grain site, e is this energy at a GB site, P the number of dopant atoms at grain sites, p the number at GB sites, N the number of grain sites, n the number of GB sites, and the configurational entropy of the dopant. Minimizing g gives:

$$\frac{p}{n-p} = \frac{P}{N-P} \exp\left(\frac{E-e}{kT}\right)$$

or

$$C_{GB} = \frac{C\, e^{Q/RT}}{1 - C + Ce^{Q/RT}}$$

where

$$C_{GB} = \frac{p}{N}\,, \quad C = \frac{P}{N}$$

$$Q\left(\frac{cal}{mol}\right) = N_A (E-e)\,.$$

The energy of segregation term, Q, is expressed in these units due to common usage. With $C \ll 1$:

$$C_{GB} = \frac{C\, e^{Q/RT}}{1 + Ce^{Q/RT}}$$

Acknowledgements

I wish to thank Ron Gronsky, my research advisor for his endless enthusiasm and encouragement, Gareth Thomas and Eugene Haller for their review of the thesis, my fellow students, in particular José Briceno-Valero for instruction on the use of the STEM, Bill Shepherd of Fairchild for the material used in this study, Ann Marshall for the use of the Stanford Materials Research Center's EM400, and Madeline Moore, typist and surrogate mother.

This work was supported by the Director, Office of Energy Research, Office of Basic Energy Sciences, Materials Science Division of the U. S. Department of Energy under Contract No. DE-AC03-76SF00098.

References

1. W. E. Taylor, N. H. Odell, and H. Y. Fan, Phys. Rev. 88, 867 (1952).
2. H. F. Matare, Defect Electronics in Semiconductors, Wiley-Interscience, New York (1971).
3. A. G. Tweet, Phys. Rev. 99, 1182 (1955).
4. T. I. Kamins, J. Appl. Phys. 42, 4357 (1971).
5. J. Y. W. Seto, J. Appl. Phys. 46, 5247 (1975).
6. G. Baccarani, B. Ricco and G. Spadini, J. Appl. Phys. 49, 5565 (1978).
7. T. I. Kamins, J. Electrochem. Soc. 127, 636 (1980).
8. M. M. Mandurah, K. C. Saraswat and T. I. Kamins, Appl. Phys. Lett. 36, 683 (1980).
9. M. M. Mandurah, K. C. Saraswat, C. R. Helms and T. I. Kamins, J. Appl. Phys. 51, 5755 (1980).
10. C. H. Seager, D. S. Ginley and J. D. Zook, Appl. Phys. Lett. 36, 831 (1980).
11. B. Swaminathan, E. Demoulin, T. W. Sigmon, R. W. Dutton and R. Reif, J. Electrochem. Soc. 127, 2227 (1980).
12. J. Budai, W. Gaudig and S. Sass, Phil. Mag. 40A, 757 (1979).
13. R. W. Balluffi, in Interfacial Segregation, W. C. Johnson and J. M. Blakely, (eds.), American Society for Metals, Metals Park, Ohio (1979), p. 193.
14. J. I. Goldstein, in Introduction to Analytical Electron Microscopy, J. J. Hren, J. I. Goldstein and D. C.Joy, (eds.), Plenum Press, New York (1979), p. 100.
15. P. Rez, private communication.
16. P. H. Pumphrey and K. M. Bowkett, Scripta Met. 5, 365 (1975).
17. H. Mykura, in Grain Boundary Structure and Kinetics, ASM Matls. Sci. Sem. 1979, ASM, Metals Park, Ohio (1980), p. 445.

18. P. H. Pumphrey, in Grain Boundary Structure and Properties, (see Ref. 20).

19. Bollmann, W., Crystal Defects and Crystalline Interfaces, Springer-Verlag, Berlin (1970).

20. G. A. Chadwick and D. A. Smith (eds.), Grain Boundary Structure and Properties, Academic Press, London (1976).

21. B. Leberg and H. Norden, ibid, p. 1.

22. A. Bourret and J. Desseaux, Phil. Mag. 39A, 405 (1979).

23. C. B. Carter, J. H. Rose and D. Ast in Microscopy of Semiconductor Materials Conference, Oxford, 6-10 April 1981, Inst. Phys. Conf. Ser. No. 60: Sec. 3.

24. R. Schindler, J. H. Rose and D. Ast, J. Metals 31(8), F-42 (1979).

25. H. Föll and D. Ast, Phil. Mag. 40, 1045 (1981).

26. J.-J. Müller, Phil. Mag. 43, 1045 (1981).

27. J. Hornstra, Phys. Chem. Solids 5, 129 (1958).

28. J.-J. Bacmann, J. P. Millier, M. Petit and G. Silvestre, Mater. Res. Bull. 15, 261 (1980).

29. J. J. Bacmann, G. Silvestre, M. Petit and W. Bollmann, Phil. Mag. 43A, 189 (1981).

30. W. Bollmann, G. Silvestre and J.-J. Bacmann, Phil. Mag. 43A, 201 (1981).

31. J. M. Briceno-Valero, Ph.D. Thesis, University of California, Berkeley (1981).

32. Y. Ishida, T. Inoue, T. Yamamoto and M. Mori, Metal Science 16, 424 (1976).

33. V. I. Fistul', Heavily Doped Semiconductors, Plenum Press, New York (1969).

34. A. J. Goss, K. E. Benson and W. G. Pfann, Acta Met. 4, 332 (1956).

35. D. McLean, Grain Boundaries in Metals, Clarendon Press, Oxford (1957).

36. R. O. Schwenker, E. S. Pan, and R. F. Lever, J. Appl. Phys. 42, 3195 (1970).

37. P. Doig and P. E. J. Flewitt, J. Micros. 112, 257 (1978).

Table I

Anneal Temperature	Anneal Time
650°C	282 hr
700°C	$19\frac{1}{2}$
750°C	$28\frac{1}{2}$
800°C	$2\frac{1}{2}$

Table II

Grain Boundary X-ray Data

(100Å Probe)

Anneal Temperature	SiK_α	PK_α (GB Excess)	σ	Concentration (monolayers)
650°C	41,430	203	49	.28
	40,436	36	46	.05
	9,400	30	28	.18
	5,471	54	21	.57
	12,196	118	29	.56
	17,403	53	35	.18
	10,003	33	26	.19
700°C	26,088	236	72	.52
	36,032	38	74	.06
	54,103	195	84	.21
	11,254	98	47	.50
	13,965	68	46	.28
	6,496	-19	29	-.17
	18,949	130	60	.40
750°C	7,559	60	18	.46
	12,619	2	22	.01
	16,081	95	27	.34
	5,462	27	14	.29
	15,589	8	25	.03
	12,190	15	21	.07
	8,242	35	18	.25
	9,632	31	21	.19
	11,975	22	23	.11
800°C	19,525	57	33	.17
	8,006	15	19	.11
	11,964	115	24	.55
	18,288	76	28	.24
	16,203	-5	29	-.02
	16,767	11	29	.04
	10,646	0	19	0
	20,632	68	30	.19

Table III

CSL/Segregation Correlation

Observed GB Type	Monolayers Segregated
Σ 11 <110>/50.5°	.17 $\pm$ .10
Σ 17 <221>/61.9°	< .24
Random	.55 $\pm$ .12
Random	.24 $\pm$ .09
Σ 3 Twin	< .09
Σ 1 (low angle)	< .15

(All 800°C anneals. See Table II)

Figure Captions

Fig. 1. Schematic view of specimen region sampled by a small electron probe.

Fig. 2. Typical X-ray spectra (smoothed) depicting a matrix spectrum (dots) and a GB spectrum (solid line).

Fig. 3. Sample Auger depth concentraiton profile, comparing the unannealed material with that annealed at 650°C for 283 hours.

Fig. 4. Typical TEM view of polysilicon, showing several grains and twins.

Fig. 5. TEM image (BF) of a low angle boundary

Fig. 6. Arrows indicate surface features appearing in chemically thinned, annealed specimens.

Fig. 7. Dislocation loops in a specimen annealed at 700°C.

Fig. 8. Arrows indicate possible phosphorus atom clusters. This specimen received the doping treatment, but was not subsequently annealed.

Fig. 9. Theoretical curve fitted to experimental points for the average degree of segregation at each temperature.

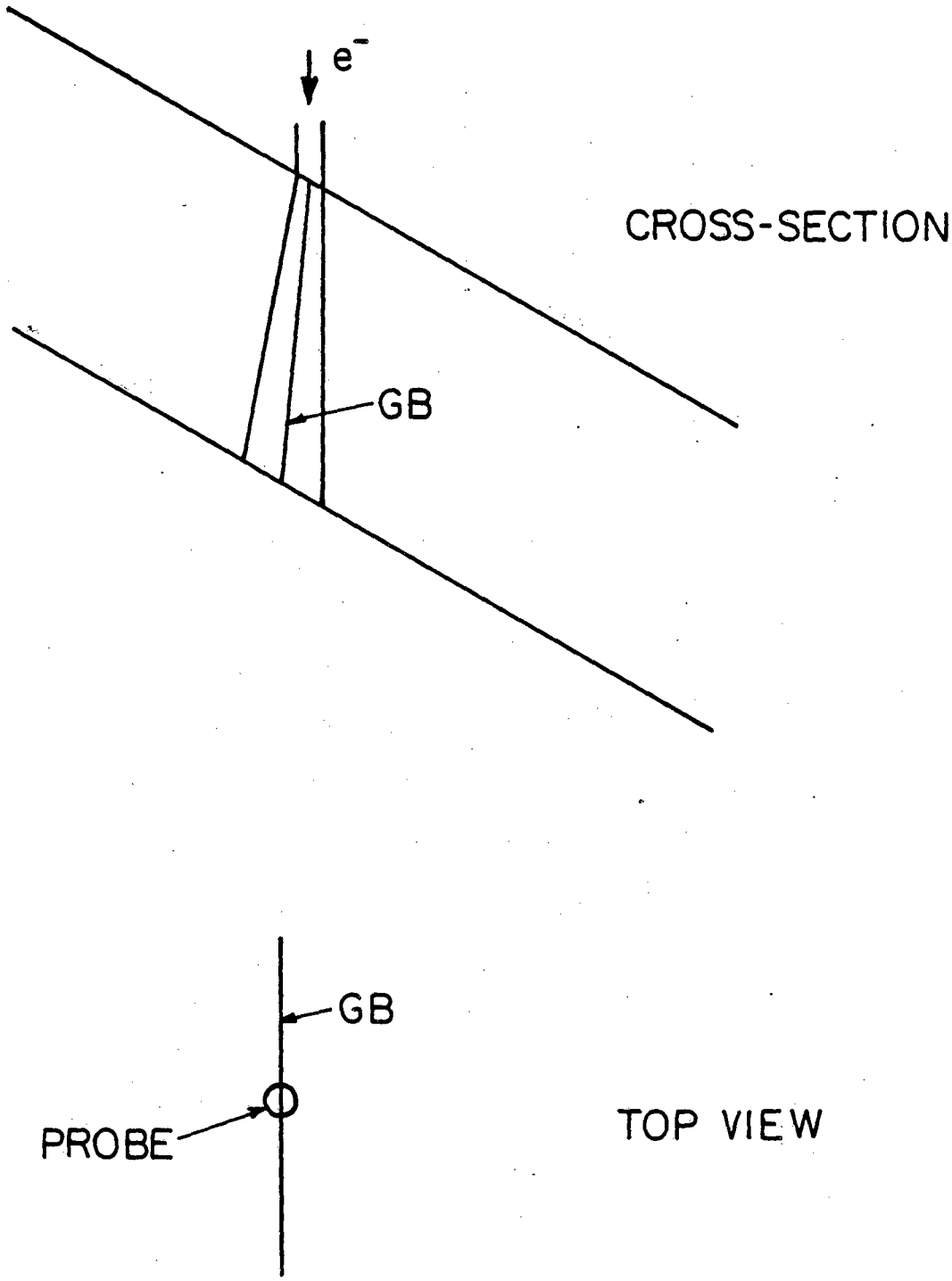

Fig. 1

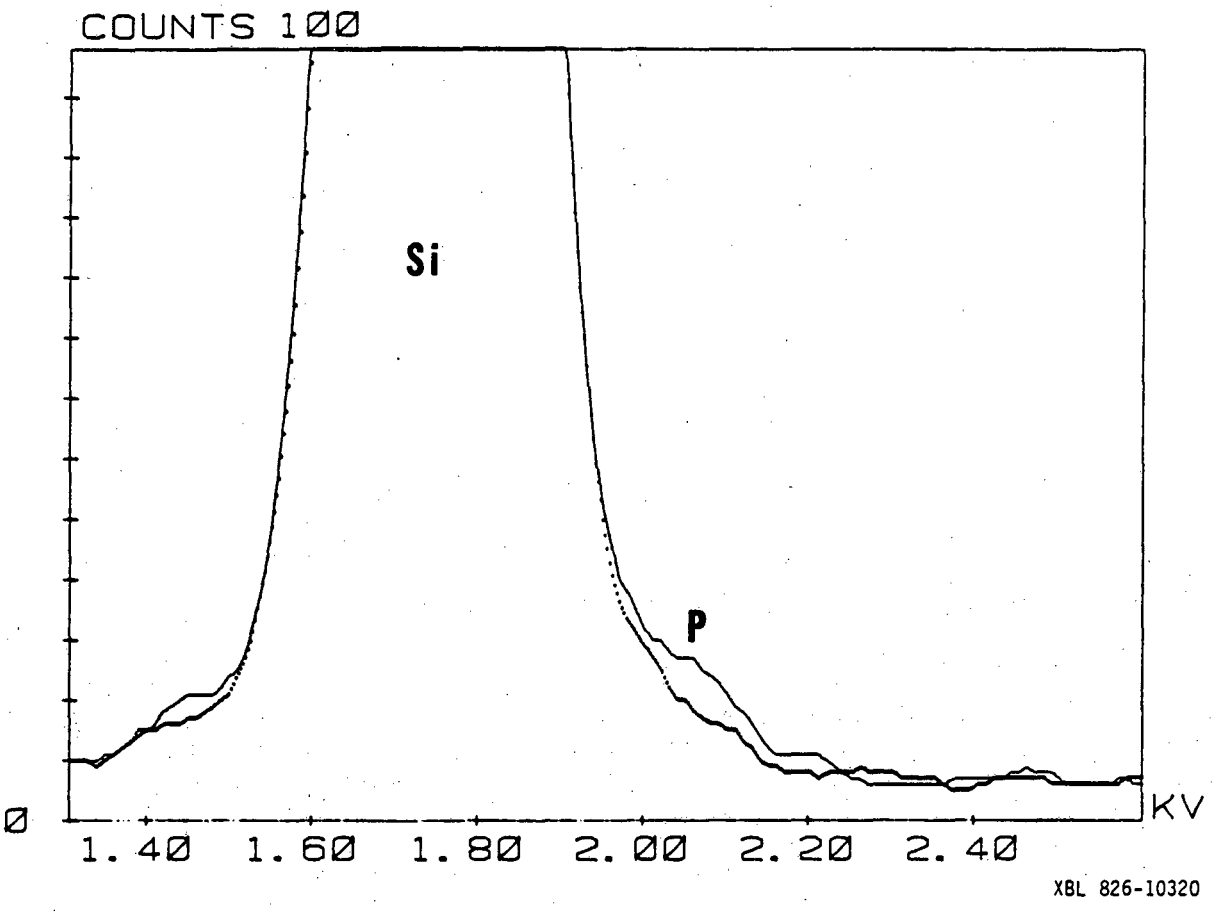

Fig. 2

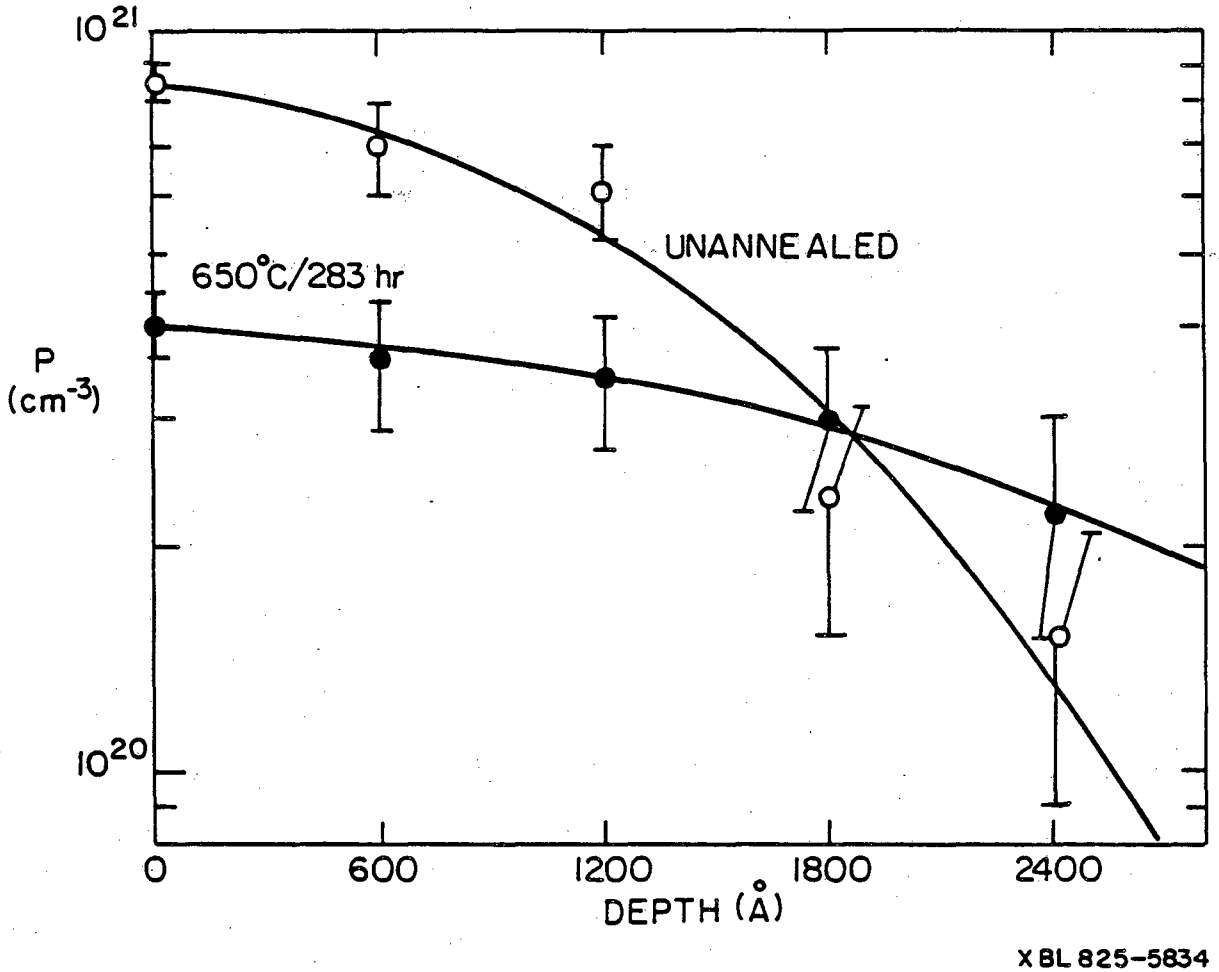
10^{21}
10^{20}
P
(cm^{-3})
650°C/283 hr
UNANNEALED
0
600
1200
1800
2400
DEPTH (Å)
XBL 825-5834

Fig.3

XBB 826-5197

Fig.4

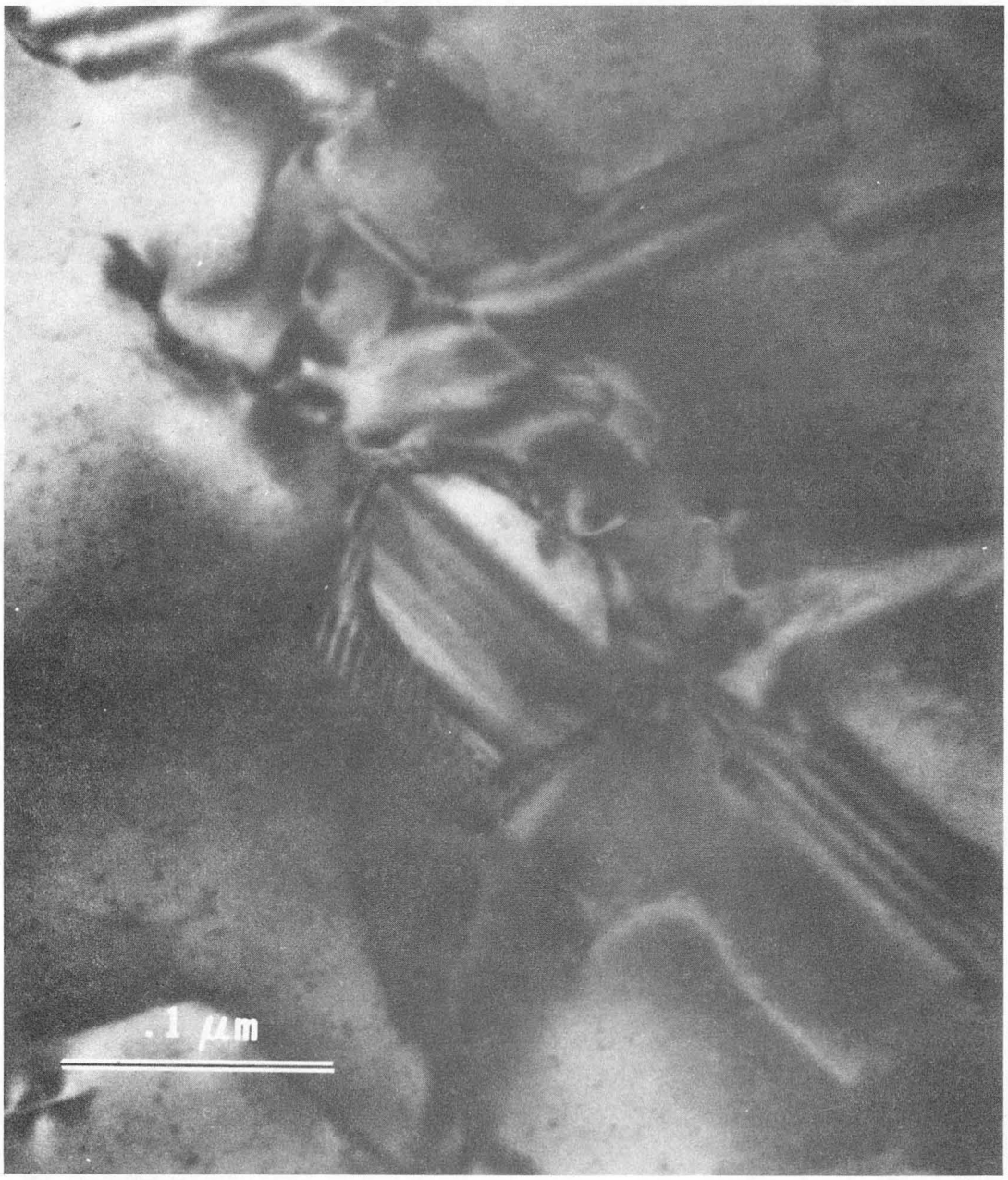

XBB 826-5196

Fig. 5

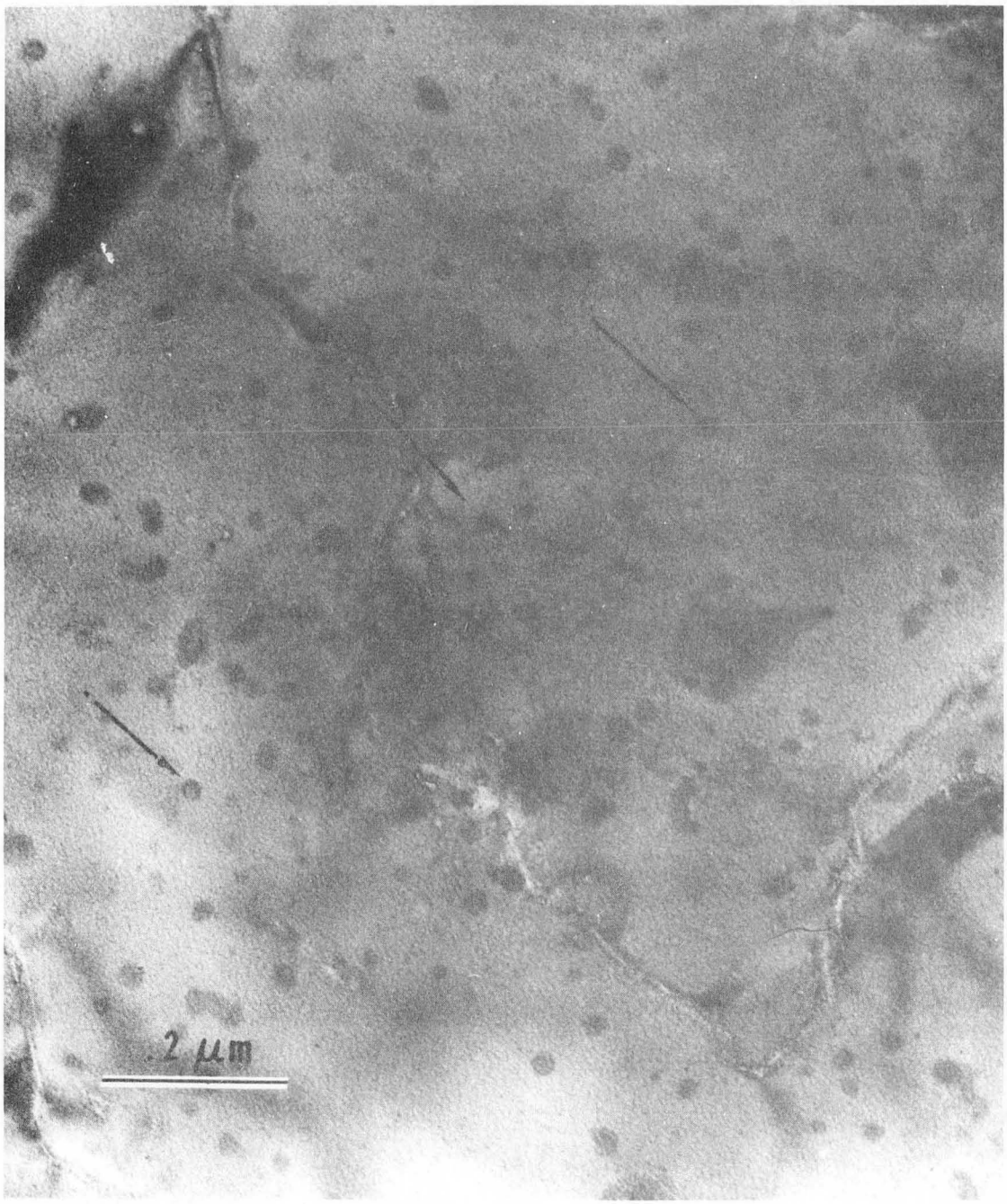

XBB 826-5195

Fig. 6

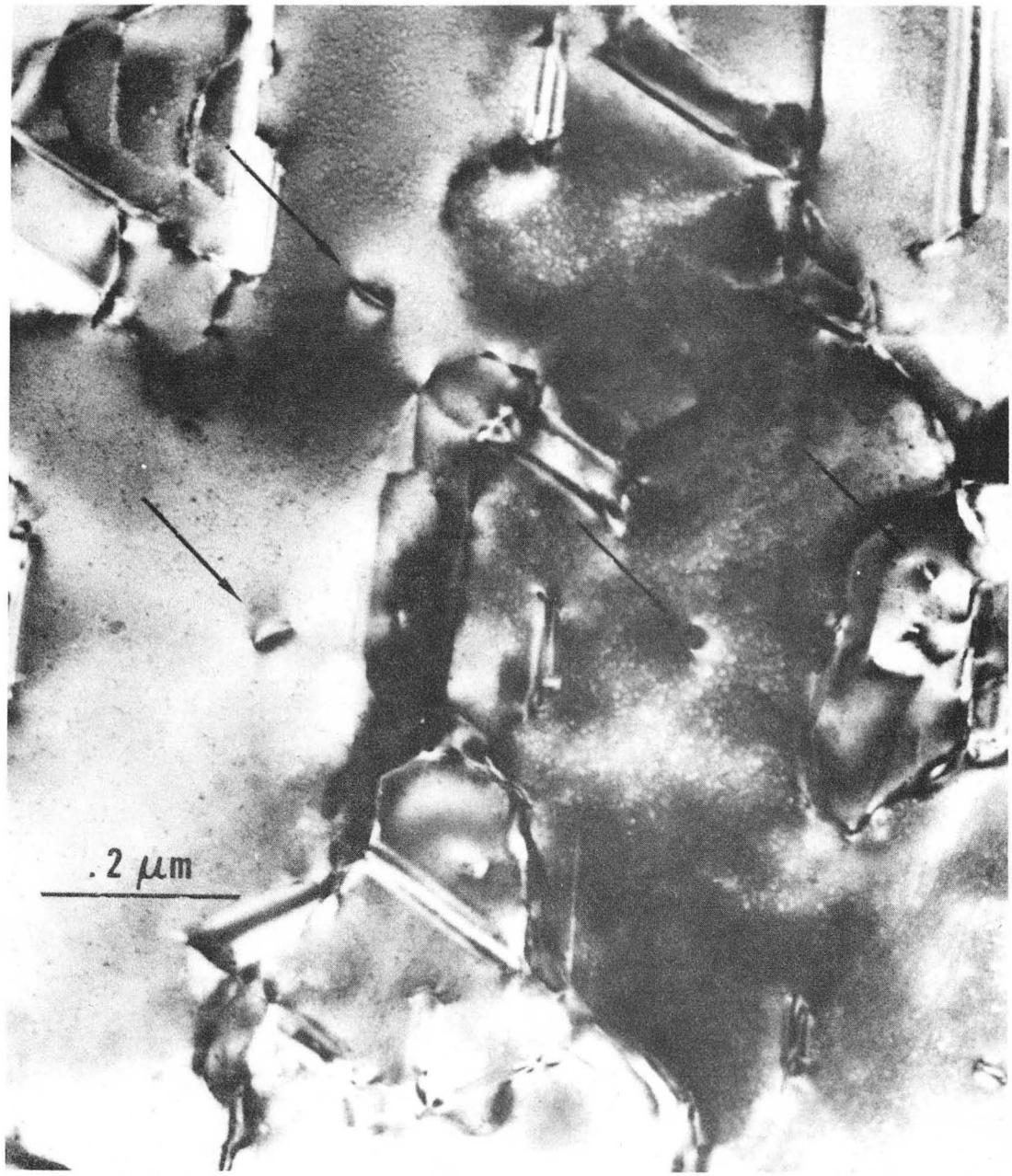

XBB 826-5194

Fig. 7

XBB 826-5193

Fig. 8

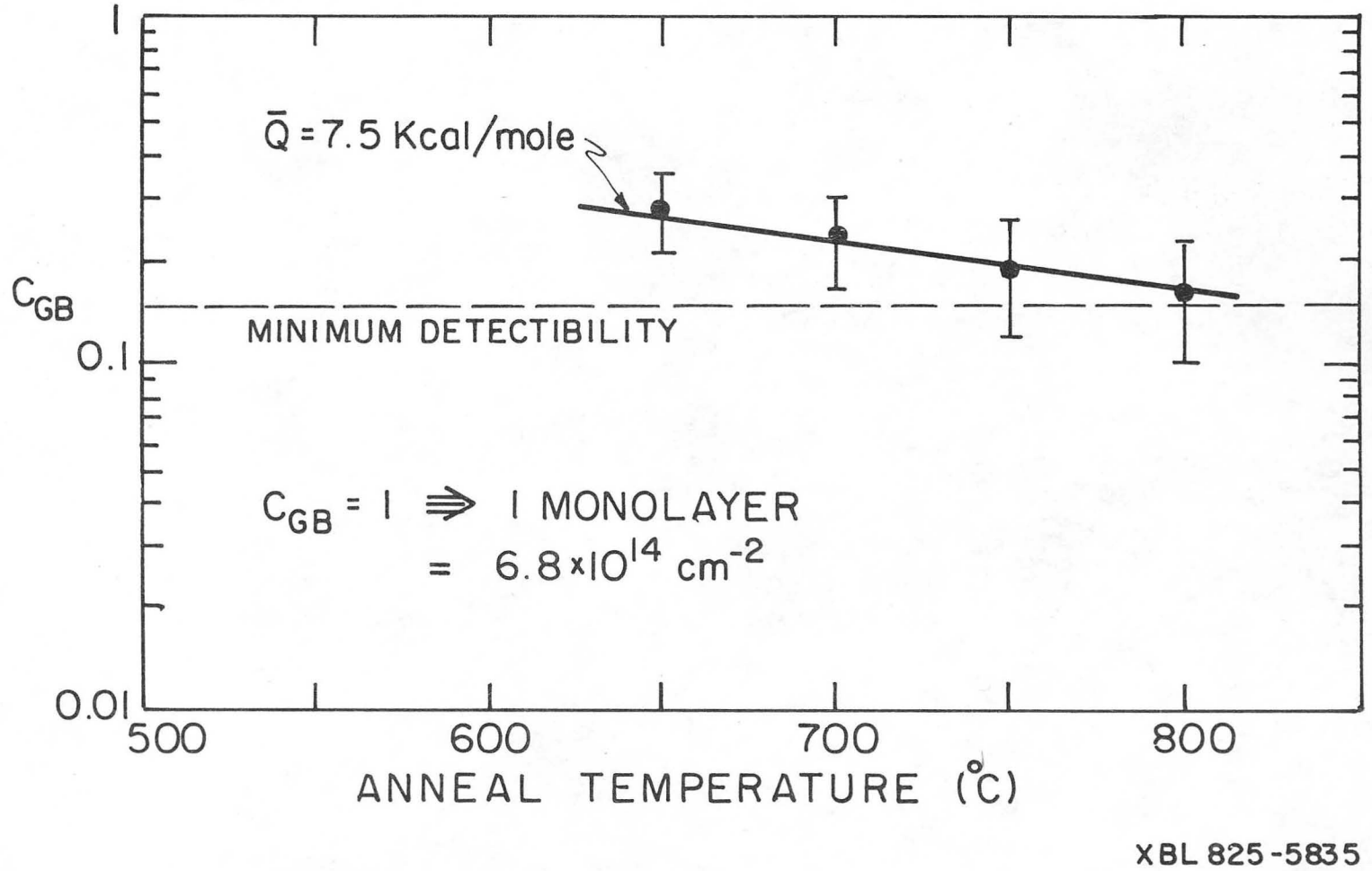
1
C_{GB}
0.1
0.01
$\bar{Q}$ = 7.5 Kcal/mole
MINIMUM DETECTIBILITY
C_{GB} = 1 ⇛ 1 MONOLAYER
= 6.8×10^{14} cm^{-2}
500
600
700
800
ANNEAL TEMPERATURE (°C)
XBL 825-5835

Fig. 9

TECHNICAL INFORMATION DEPARTMENT
LAWRENCE BERKELEY LABORATORY
UNIVERSITY OF CALIFORNIA
BERKELEY, CALIFORNIA 94720